Draft 3
July 10, 2008

CMS Search Plans and Sensitivity to New Physics with Dijets

The CMS Collaboration

Abstract

CMS will use dijets to search for physics beyond the standard model during early LHC running. The inclusive jet cross section as a function of jet transverse momentum, with 10 pb^{-1} of integrated luminosity, is sensitive to contact interactions beyond the reach of the Tevatron. The dijet mass distribution will be used to search for dijet resonances coming from new particles, for example an excited quark. Additional sensitivity to the existence of contact interactions or dijet resonances can be obtained by comparing dijet rates in two distinct pseudorapidity regions.

The Large Hadron Collider at CERN will produce many events with two energetic jets resulting from proton-proton collisions at $\sqrt{s} = 14$ TeV. These dijet events result from parton scattering, produced by the strong interaction of quarks (q) and gluons (g) inside the protons. This paper discusses plans to use dijets in the search for two signals of new physics: contact interactions and resonances decaying into dijets. This generic search is applied to two models of quark compositeness, that are used as benchmarks of sensitivity to new physics. The first model is a contact interaction [1] among left-handed quarks at an energy scale Λ^+ in the process $qq \to qq$, modeled with the effective Lagrangian $L_{qq} = (\pm 2\pi/\Lambda^2)(\overline{q}_L \gamma^\mu q_L)(\overline{q}_L \gamma_\mu q_L)$ with + chosen for the sign. The second model is an excited quark (q^*) [2] in the process $qg \to q* \to qg$, detectable as a dijet resonance. All processes presented here have been simulated using PYTHIA version 6.4 [3].

A detailed description of the Compact Muon Solenoid (CMS) experiment can be found elsewhere [4, 5]. The CMS coordinate system has the origin at the center of the detector, z-axis points along the beam direction toward the Jura mountains, transverse plane perpendicular to the beam, azimuthal angle ϕ, polar angle θ, and pseudorapidity $\eta = -\ln(\tan[\theta/2])$. The central feature of the CMS apparatus is a superconducting solenoid, of 6 m internal diameter. Within the field volume are the silicon pixel and strip tracker, and the barrel and endcap calorimeters ($|\eta| < 3$): a crystal electromagnetic calorimeter (ECAL) and a brass-scintillator hadronic calorimeter (HCAL). Outside the field volume, in the forward region, there is an iron-quartz fiber hadronic calorimeter ($3 < |\eta| < 5$). The HCAL and ECAL cells are grouped into towers, projecting radially outward from the origin, for triggering purposes and to facilitate the jet reconstruction. In the region $|\eta| < 1.74$ these projective calorimeter towers have segmentation $\Delta\eta = \Delta\phi = 0.087$, and the η and ϕ width progressively increases at higher values of η. The energy in the HCAL and ECAL within each projective tower is summed to find the calorimeter tower energy. Towers with $|\eta| < 1.3$ contain only cells from the barrel calorimeters, towers in the transition region $1.3 < |\eta| < 1.5$ contain a mixture of barrel and endcap cells, and towers in the region $1.5 < |\eta| < 3.0$ contain only cells from the endcap calorimeters.

Jets are reconstructed using both the iterative and midpoint cone algorithms [5], with indistinguishable results for this analysis. Below we will discuss three types of jets: reconstructed, corrected and generated. The reconstructed jet energy, E, is defined as the scalar sum of the calorimeter tower energies inside a cone of radius $\sqrt{(\Delta\eta)^2 + (\Delta\phi)^2} = 0.5$, centered on the jet axis. The jet momentum, $\vec{p}$, is the corresponding vector sum: $\vec{p} = \sum E_i \hat{u}_i$ with $\hat{u}_i$ being the unit vector pointing from the origin to the energy deposition E_i inside the same cone. The jet transverse momentum, p_T, is the component of $\vec{p}$ in the transverse plane. The E and $\vec{p}$ of a reconstructed jet are then corrected for the non-linear response of the calorimeter to a generated jet. Generated jets come from applying the same jet algorithm to the Lorentz vectors of stable generated particles before detector simulation. On average, the p_T of a corrected jet is equal to the p_T of the corresponding generated jet. The corrections estimated from a GEANT [6] simulation of the CMS detector increase the average jet p_T by roughly 50% (10%) for 70 GeV (3 TeV) jets in the region $|\eta| < 1.3$. Further details on jet reconstruction and jet energy corrections can be found elsewhere [5, 7]. The jet measurements presented here are within the region $|\eta| < 1.3$, where the sensitivity to new physics is expected to be the highest, and where the reconstructed jet response variations as a function of η are both moderate and smooth.

The dijet system is defined to be composed of the two jets with the highest p_T in an event (leading jets), and the dijet mass is given by $m = \sqrt{(E_1 + E_2)^2 - (\vec{p}_1 + \vec{p}_2)^2}$. The estimated dijet mass resolution varies from 9% at a dijet mass of 0.7 TeV to 4.5% at 5 TeV.

CMS will record events that pass a first level trigger and a high level trigger. For an instantaneous luminosity of 10^{32} cm^{-2}s^{-1}, consider three event samples collected by requiring at least one jet in the high level trigger with corrected transverse energy above 60, 120 and 250 GeV, prescaled by factors of 2000, 40 and 1, respectively. For an integrated luminosity of 100 pb^{-1}, the three event samples will effectively correspond to 0.05, 2.5, and 100 pb^{-1}. The first event sample will be used to measure the trigger efficiency of the second sample. The second and third event samples will be used to study dijets of mass above 330 and 670 GeV, respectively, where the trigger efficiencies are expected to be higher than 99% [8].

Backgrounds from cosmic rays, beam halo, and detector noise are expected to occasionally produce events with large or unbalanced energy depositions. They will be removed by requiring $\not{E}_T / \sum E_T < 0.3$ and $\sum E_T < 14$ TeV, where $\not{E}_T$ ($\sum E_T$) is the magnitude of the vector (scalar) sum of the transverse energies measured by all calorimeter towers in the event. This cut is estimated to be more than 99% efficient for both QCD jet events and the signals of new physics considered. In the high p_T region relevant for this search, jet reconstruction is fully efficient.

CMS plans to search for contact interactions using the jet p_T distribution. Figure 1 shows the inclusive jet differential cross section as a function of p_T, for jets with $|\eta| < 1$. Considering first the QCD processes, the reconstructed and corrected quantities are compared with the QCD prediction for generated jets. After corrections, the reconstructed and generated distributions agree. The ratio of the corrected jet cross section to the generated jet cross section varies between 1.2 at $p_T = 100$ GeV and 1.05 at $p_T = 500$ GeV, remaining roughly constant for higher p_T. The deviation of this ratio from 1 is attributed to the smearing effect of the jet p_T resolution on the steeply falling spectrum. The measured spectrum could be further corrected for resolution smearing, and this ratio from Monte Carlo is an estimate of the size of that correction. The measurement uncertainties are predominantly systematic. The inset in Figure 1 shows the effect on the jet rate of a 10% uncertainty in the jet energy correction. This level of uncertainty could be expected in early running, for an integrated luminosity around 10 pb^{-1}. This experimental uncertainty is roughly ten times larger than the uncertainties from parton distributions, as estimated using CTEQ6.1 fits [9]. Figure 1 shows that the effect of new physics from a contact interaction with scale $\Lambda^+ = 3$ TeV is convincingly above what could be expected for measurement uncertainties with only 10 pb^{-1}. For comparison, a Tevatron search has excluded contact interactions with scales Λ^+ below 2.7 TeV [10].

CMS plans to search for narrow dijet resonances using the dijet mass distribution. Figure 2 shows the differential cross section versus dijet mass, where both leading jets have $|\eta| < 1$, and the mass bins have a width roughly equal to the dijet mass resolution. Considering first the QCD processes, the cross section for corrected jets agrees with the QCD prediction from generated jets. To determine the background shape either the Monte Carlo prediction or a parameterized fit to the data can be used. The inset to Figure 2 shows a simulation of narrow dijet resonances with a q^* production cross section. This is compared to the QCD statistical uncertainties, including trigger prescaling. This shows that with an integrated luminosity of 100 pb^{-1} a q^* dijet resonance with a mass of 2 TeV would produce a convincing signal above the statistical uncertainties from the QCD background. For comparison, a Tevatron search has excluded q^* dijet resonances with mass, M, below 0.87 TeV [11]. The heaviest dijet resonances that CMS can discover (at five standard deviations) with 100 pb^{-1} of integrated luminosity, using this search technique and including the expected systematic uncertainties [12, 13], are: 2.5 TeV for q^*, 2.2 TeV for axigluons [14] or colorons [15], 2.0 TeV for E_6 diquarks [16], and 1.5 TeV for color octet technirhos [17]. Studies of the jet η cut have concluded that the optimal sensitivity to new physics is achieved with $|\eta| < 1.3$ for a 2 TeV spin 1 dijet resonance decaying to $q\bar{q}$ [18].

CMS plans to search for both contact interactions and dijet resonances using the dijet ratio, $r = N(|\eta| < 0.7)/N(0.7 < |\eta| < 1.3)$, where N is the number of events with both jets in the specified $|\eta|$ region. The dijet ratio is sensitive to the dijet angular distribution. For the QCD processes, the dijet ratio is the same for corrected jets and generated jets, and is constant at $r = 0.5$ for dijet masses up to 6 TeV [18]. Figure 3 shows the dijet ratio from contact interactions and dijet resonances, compared to the expected statistical uncertainty on the QCD processes, for 100 pb^{-1} of integrated luminosity, including trigger prescaling. The signal from a contact interaction with scale $\Lambda^+ = 5$ TeV rises well above the QCD statistical errors at high dijet mass. Systematic uncertainties in the dijet ratio are expected to be small, since they predominantly cancel in the ratio as previously reported [12, 19]. Using the dijet ratio, CMS can discover a contact interaction at scale $\Lambda^+ = 4$, 7 and 10 TeV with integrated luminosities of 10, 100, and 1000 pb^{-1}, respectively [18]. The signal from a 2 TeV spin 1/2 q^* produces a convincing peak in the dijet ratio, because it has a significant rate and a relatively isotropic angular distribution compared to the QCD t-channel processes. Fixing the cross section of the 2 TeV dijet resonance for $|\eta| < 1.3$ at 13.6 pb (from the q^* model), the dijet ratio in the presence of QCD background increases by approximately 6% when considering a spin 2 resonance decaying to both $q\bar{q}$ and gg (such as a Randall-Sundrum graviton [20]), and the dijet ratio decreases by approximately 4% when considering a spin 1 resonance decaying to $q\bar{q}$ (such as a Z$'$, axigluon, or coloron) [18]. Hence, the sensitivity to a 2 TeV dijet resonance depends only weakly on the spin of the resonance. Nevertheless, with sufficient luminosity, this simple measure of the dijet angular distribution, or a more complete evaluation of the angular distribution, can be used to see these small variations and infer the spin of a dijet resonance.

In conclusion, CMS plans to use measurements of rate as a function of jet p_T and dijet mass, as well as a ratio of dijet rates in different η regions, to search for new physics in the data sample collected during early LHC running. With integrated luminosity samples in the range 10–100 pb^{-1}, CMS will be sensitive to contact interactions and dijet resonances beyond those currently excluded by the Tevatron.

We thank the technical and administrative staffs at CERN and other CMS Institutes, and acknowledge support from: FMSR (Austria); FNRS and FWO (Belgium); CNPq and FAPERJ (Brazil); MES (Bulgaria); CERN; CAS and NSFC (China); MST (Croatia); University of Cyprus (Cyprus); Academy of Sciences and NICPB (Estonia); Academy of Finland, ME and HIP (Finland); CEA and CNRS/IN2P3 (France); BMBF and DESY (Germany); GSRT (Greece); NKTH (Hungary); DAE and DST (India); IPM (Iran); UCD (Ireland); INFN (Italy); KICOS (Korea); CINVESTAV, CONACYT and UASLP-FAI (Mexico); PAEC (Pakistan); SCSR (Poland); FCT (Portugal); JINR (Armenia, Belarus, Georgia, Ukraine, Uzbekistan); MST and MAE (Russia); MSEP (Serbia); OCT (Spain); ETHZ, PSI, University of Zurich (Switzerland); NSC (Taipei); TUBITAK and TAEK (Turkey); STFC (United Kingdom); DOE and NSF (USA).

References

[1] E. Eichten, K. Lane and M. E. Peskin, Phys. Rev. Lett. **50**, 811 (1983).

[2] U. Baur, I. Hinchliffe and D. Zeppenfeld, Int. J. Mod. Phys. **A2**, 1285 (1987).

[3] T. Sjostrand, L. Lonnblad, S. Mrenna, hep-ph/0108264.

[4] CMS Collaboration, "The CMS experiment at the CERN LHC" (accepted for publication in JINST).

[5] CMS Collaboration, Physics TDR Volume I, CERN-LHCC-2006-001.

[6] S. Agostinelli *et al.* (GEANT4 Collaboration), Nucl. Instrum. Meth. A**506**, 250 (2003).

[7] CMS Collaboration, CMS Physics Analysis Summary JME-07-003 (2008). at http://cms-physics.web.cern.ch/cms-physics/public/JME-07-003-pas.pdf .

[8] S. Esen and R. Harris, CMS Note 2006/069.

[9] J. Pumplin *et al.* (CTEQ Collaboration), JHEP **07**, 012 (2002).

[10] B. Abbott *et al.* (D0 Collaboration), Phys. Rev. Lett. **82**, 2457 (1999).

[11] K. Hatakeyama *et al.* (CDF Collaboration) recent public results at http://www-cdf.fnal.gov/physics/exotic/r2a/20080214.mjj_resonance_1b/.

[12] CMS Collaboration, J. Phys. G: Nucl. Part. Phys. **34**, 995 (2006).

[13] K. Gumus, N. Akchurin, S. Esen and R. Harris, CMS Note 2006/070.

[14] J. Bagger, C. Schmidt and S. King, Phys. Rev. D**37**, 1188 (1988).

[15] E. Simmons, Phys. Rev. D**55**, 1678 (1997).

[16] J. Hewett and T. Rizzo, Phys. Rep. **183**, 193 (1989) and references therein.

[17] K. Lane and S. Mrenna, Phys. Rev. D**67**, 115011 (2003).

[18] CMS Collaboration, CMS Physics Analysis Summary SBM-07-001 (2007) at http://cms-physics.web.cern.ch/cms-physics/public/SBM-07-001-pas-v3.pdf .

[19] S. Esen and R. Harris, CMS Note 2006/071.

[20] L. Randall and R. Sundrum, Phys. Rev. Lett. **83**, 3370 (1999).

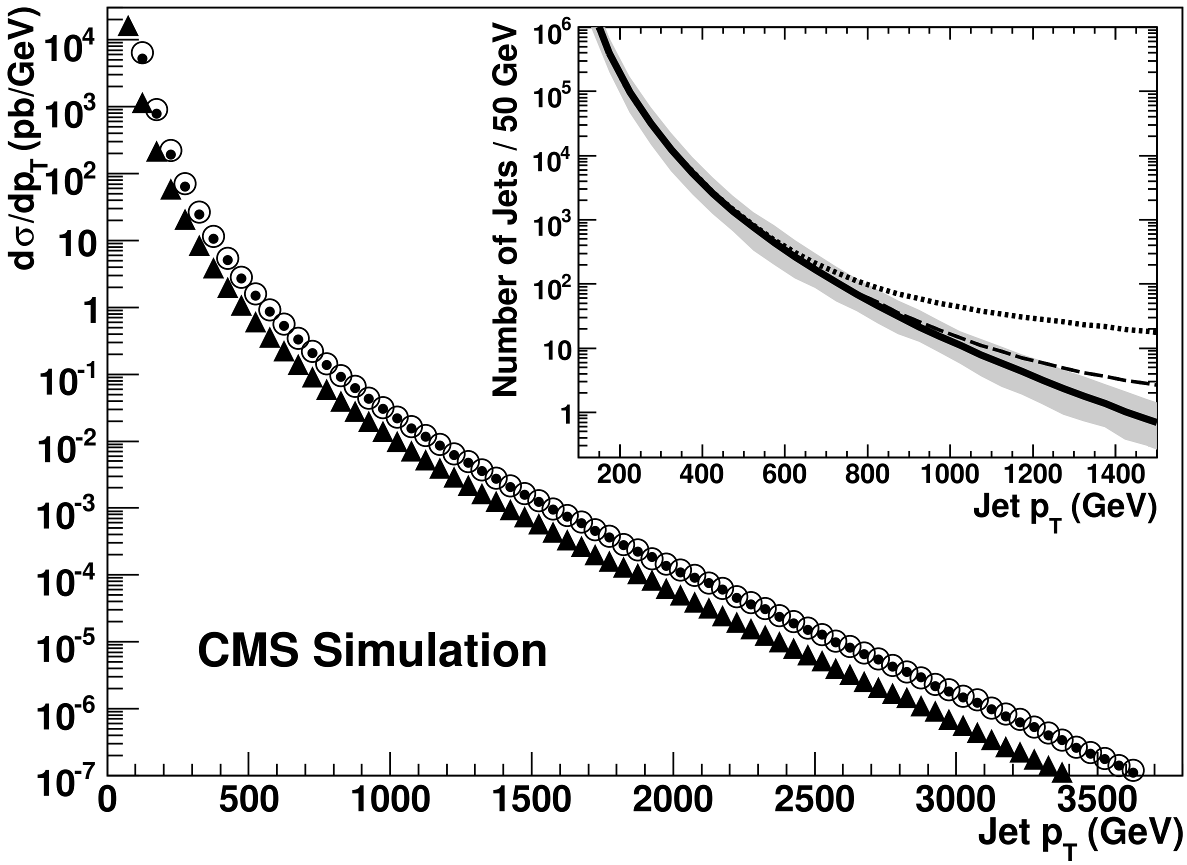

Figure 1: The inclusive jet p_T differential cross section expected from QCD for $|\eta| < 1$, for generated jets (points), reconstructed jets (triangles), and corrected jets (open circles). The inset shows the number of generated jets expected in 50 GeV bins for an integrated luminosity of 10 pb^{-1}. The standard QCD curve (solid) is modified by a signal from contact interactions with scale $\Lambda^+ = 3$ TeV (dotted) and 5 TeV (dashed). The shaded band represents the effect of a 10% uncertainty on the jet energy scale.

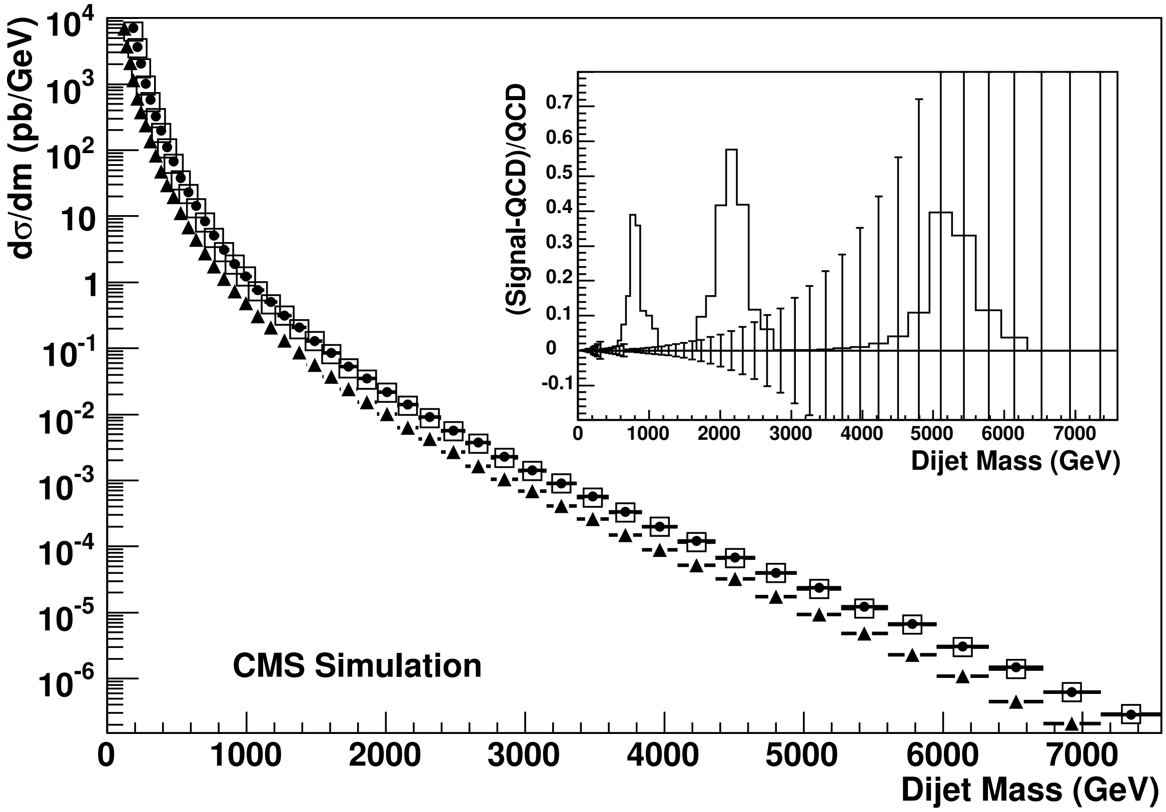

Figure 2: The dijet mass differential cross section expected from QCD for $|\eta| < 1$ from generated jets (points), reconstructed jets (triangles), and corrected jets (open boxes). The inset shows dijet resonances reconstructed using corrected jets, coming from q^* signals [13] of mass 0.7, 2, and 5 TeV. The fractional difference (histogram) between the q^* signal and the QCD background is compared to the QCD statistical error (vertical bars) for an integrated luminosity of 100 pb^{-1}.

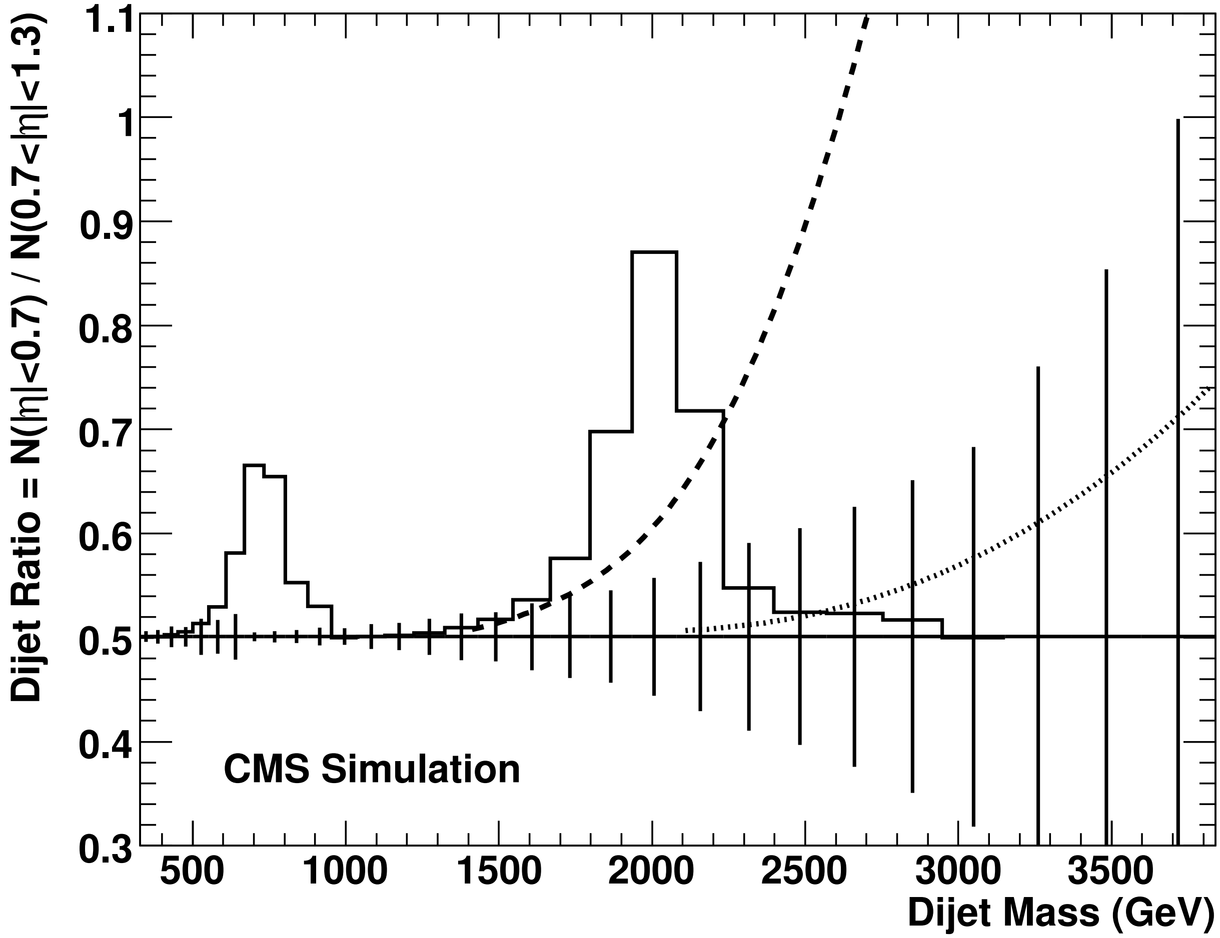

Figure 3: The dijet ratio for corrected jets expected from QCD (horizontal line), with statistical uncertainties (vertical bars) for an integrated luminosity of 100 pb^{-1}, is compared to QCD + contact interaction signals with a scale $\Lambda^+ = 5$ TeV (dashed) and 10 TeV (dotted), as well as to QCD + dijet resonance signals (histogram) with q^* masses of 0.7 and 2 TeV.